EFFECT OF SINTERING TEMPERATURE ON MICROSTRUCTURE AND MECHANICAL PROPERTIES OF AE42 MAGNESIUM ALLOY PREPARED BY SPARK PLASMA SINTERING

Peter MINÁRIK [1], František LUKÁČ [2], Jakub CINERT [2], Stanislav ŠAŠEK [1], Robert KRÁL [1]

[1] *Charles University, Department of Physics of Materials, Ke Karlovu 5, 12116 Prague, Czech Republic, EU, peter.minarik@mff.cuni.cz*

[2] *Institute of Plasma Physics, Czech Academy of Science, Za Slovankou 3, 18200 Prague, Czech Republic, EU*

Abstract

Magnesium alloy AE42 was prepared by powder metallurgy technique of spark plasma sintering. The effect of sintering parameters, particularly sintering temperature, on the microstructure and mechanical strength was investigated. The gas-atomized powder was sintered at four temperatures in the temperature range of 400-550 °C. It was found that mechanical strength of the sintered samples was significantly affected by several microstructural features. Application of relatively high load during sintering caused deformation of the individual particles and consequent recrystallization depending on the processing temperature resulted in the release of internal strain and in grain growth. As a result, the evolution of the mechanical strength as a function of the sintering temperature was significantly affected by residual stress, grain size and coarsening of secondary phase particles.

Keywords: Magnesium, spark plasma sintering, microstructure, mechanical properties

1. INTRODUCTION

Utilization of magnesium alloys increases in many sectors of industry and there is an intensive research regarding further improvement of magnesium-based materials. Powder metallurgy was found to be very effective manufacturing approach, which help to overcome formability issues, enables good control of the final microstructure and complex shapes of the product with only minimum waste could be produced [1,2]. Today, a variety of sintering techniques have been developed, from which spark plasma sintering (SPS) is one of the most effective [3]. This technique was used to prepare a wide range of pure metals and alloys including magnesium, e.g. [4-13]. It was shown that full density (>99%) could be achieved using sintering temperatures from 360-550 °C. Nevertheless, the final microstructure and also resulting mechanical properties are significantly dependent on the sintering conditions for each alloy separately. In this investigation, a commercial creep resistant magnesium alloy AE42 was used. We have already shown that sintering temperature during SPS has a major effect on the secondary phase particles distribution, but the other microstructural features were almost similar within the sintering temperature range of 450-550 °C [11]. In this work, the much higher pressure was applied during the sintering and also the range of the sintering temperature was extended.

2. MATERIALS AND METHODS

Gas atomized powder of commercial AE42 (Mg-4Al-2RE) was supplied form TU Clausthal, Germany. Powder particles of size <80 μm were sintered using spark plasma sintering (SPS) system - type 10-4, Thermal technology LLC. Sintering was performed at four temperatures - 400 °C, 450 °C, 500 °C and 550 °C. The temperature was measured by a thermocouple placed in the graphite tooling in the vicinity of the sample. Two hold times were used in this study. Hold time of 10 min was used for temperatures 400 and 450 °C and 3 min was used for temperatures 500 and 550 °C. Prolonged hold time used for lower temperatures was selected in order to ensure sufficiently high density of the final product. The mechanical load was continuously increased

during heating to its maximum value of 100 MPa and was held during the sintering period. Afterwards, the load was released together with rapid cooling of the sintered sample.

The microstructure of the initial powder and compacted samples were studied by scanning electron microscope (SEM) ZEISS Auriga Compact equipped with EDAX electron backscatter diffraction (EBSD) camera. Samples for SEM observation were mechanically polished down to 60 nm alumina solution. Subsequent ion-polishing by Leica EM RES120 system was used prior to EBSD measurement. The raw data from EBSD measurement were processed in OIM TSL 7 software, as described in detail elsewhere [14]. For each sample, four scans of 300x300 μm were performed in order to acquire sufficient statistics.

Microhardness of the sintered samples was investigated by fully automated system QNESS Q10 equipped with a Vickers indenter. Samples for the measurement were prepared similarly as for SEM observation. At least 50 indents were measured for each sample in order to achieve sufficient statistic.

3. RESULTS AND DISCUSSION

Figure 1a shows shape and size distribution of the atomized powder particles prior to the sintering and **Figure 1b** shows their microstructure in cross-section. Powder particles had mostly ellipsoidal shape and their size distribution was rather wide. Their microstructure dominated the eutectic lamellar structure of secondary phases. Combination of energy-dispersive X-ray spectroscopy and X-ray diffraction showed that these secondary phase particles are $Al_{11}RE_3$ and/or Al_2RE [11]. The grain structure of these initial powder particles was highly dependent on the individual particle. High cooling rates during solidification resulted in irregular grain structure, when most of the particles contained one large grain filling up approximately half of the volume and plenty of small ones filling the second half, for details see [11].

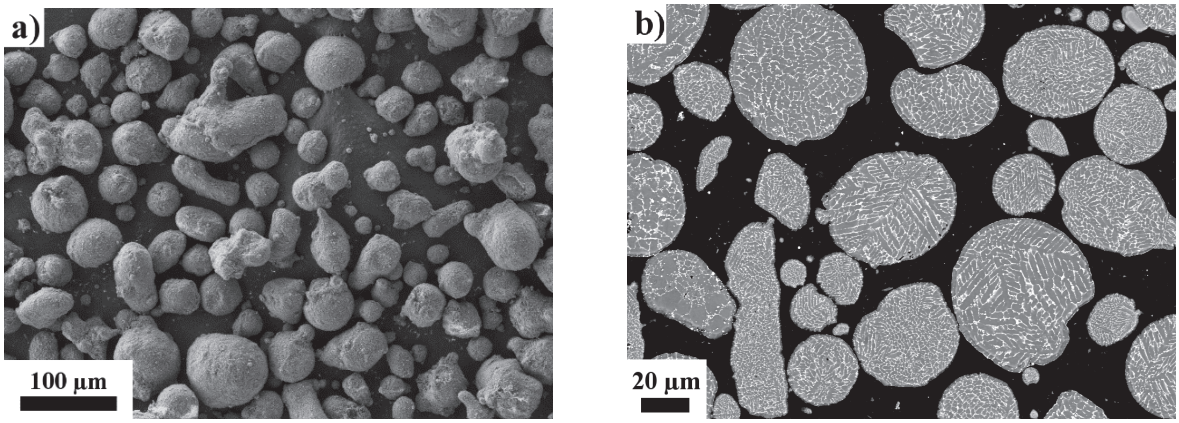

Figure 1 As received powder particles - (a) size and morphology and (b) microstructure (SEM)

Four samples were sintered from the initial powder using sintering temperature in the range of 400-550 °C. Density determination by pycnometer revealed that almost full relative density (>98%) was achieved in all samples. Nevertheless, significant differences in the microstructure were observed between the individual samples. **Figure 2** shows results of EBSD analysis, where inverse pole figure maps are presented. Calculated average grain size is shown for each sample in **Table 1**.

Sintering temperature and hold time are considered to belong to the most important parameters of SPS. Exposure to higher temperature results in faster diffusion and sintering itself is more effective. On the other hand, application of high temperature usually results in coarsening of the microstructure and, as reported previously, into coarsening of fine particles and precipitates [4,11,14]. This is often not welcome, especially with regard to the mechanical properties. In this report, the effect of sintering temperature on the mechanical

properties was studied by means of microhardness. The results are shown in **Figure 3** and clearly indicate that continuous increase of sintering temperature results in continuous loss of mechanical strength.

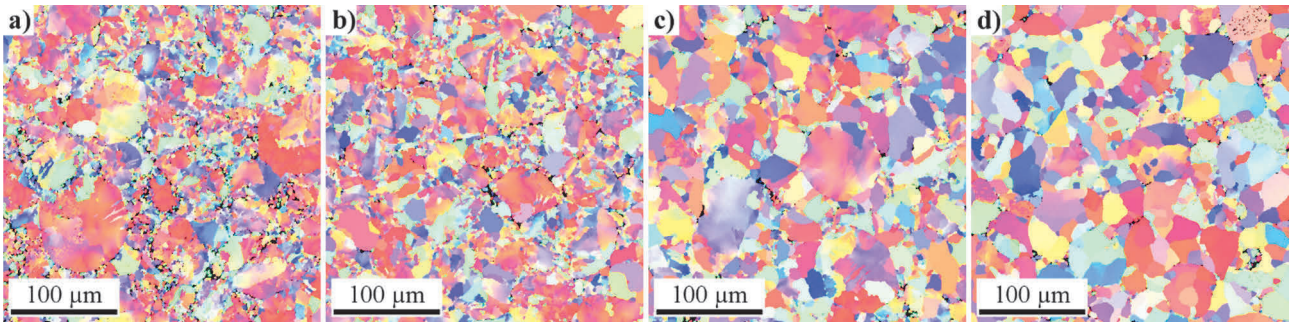

Figure 2 EBSD IPF maps of samples sintered at (a) 400 °C, (b) 450 °C, (c) 500 °C and (d) 550 °C

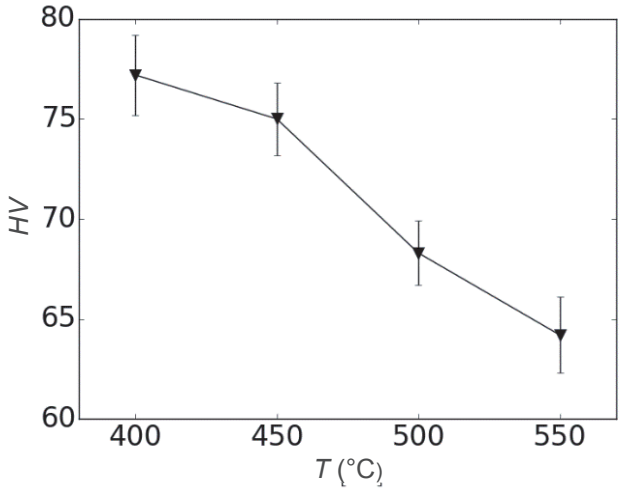

Figure 3 Evolution of microhardness as a function of sintering temperature

Deterioration of the microhardness with increasing temperature could be directly attributed to the microstructural changes in the material. In our previous report, the effect of the sintering temperature on the microstructure and mechanical properties was studied as well, however, such decrease of mechanical strength was not observed [11]. The main difference between these two studies was in the magnitude of applied load during sintering. 80 MPa used in that study did not cause major changes in the microstructure through residual stress or recrystallization, nor statistically significant change in the average grain size was measured. The only difference in the microstructure between the individual samples was coarsening of the fine lamellar structure, which caused measurable loss of the mechanical strength. Similar coarsening of was observed in samples sintered with a load of 100 MPa as well (not shown here). However, in this study more pronounced drop of microhardness was observed between the two limit temperatures and the change was almost continuous. Origin of such deterioration stems from the simultaneous evolution of other microstructural features besides secondary phase particles coarsening. This assumption is particularly relevant with regard to the evolution of average grain size. The abrupt change of microhardness between 450 and 500 °C could be associated to the sudden increase of average grain size in the same temperature region, however, the grain size evolution doesn't correlate with the other two parts of microhardness evolution.

In order to attain deeper knowledge about the microstructure evolution, grain boundary maps, kernel average misorientation (KAM) maps and grains with misorientation spread < 1.5° are shown in **Figure 4**. Additionally, characteristic parameters as a fraction of small grains (< 5 µm), a fraction of high angle grain boundaries

(HAGB) and a fraction of grains with grain orientation spread (GOS) < 1.5° was calculated from each measured EBSD dataset and the resulting average values are shown in **Table 1**.

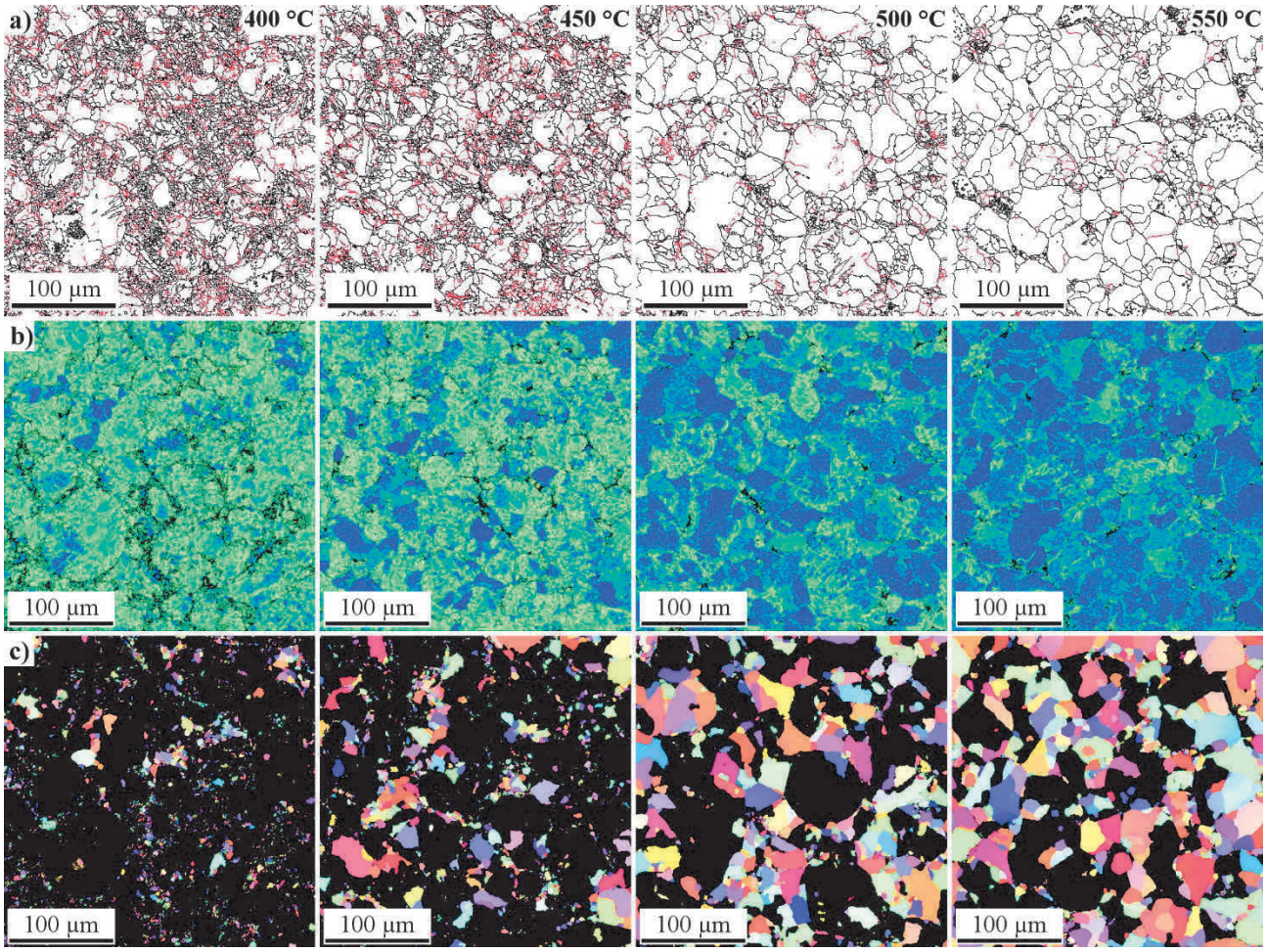

Figure 4 Maps calculated from EBSD data. (a) grain boundary map (misorientation > 15° - black, < 15° - red), (b) KAM map (0° (blue) - 5° (red)) and (c) grains with GOS < 1.5°

Table 1 Evolution of average grain size, microhardness, a fraction of grains with size < 5 µm, HAGB and grains with GOS < 1.5° as a function of sintering temperature

T (°C)	***GS*** (µm)	***HV***	***GS* < 5 µm** (%)	***HAGB*** (%)	***GOS* < 1.5°** (%)
400	17 ± 1	77 ± 2	14 ± 1	36 ± 1	9 ± 2
450	17 ± 2	75 ± 2	11 ± 1	47 ± 4	24 ± 2
500	22 ± 2	68 ± 2	7 ± 1	59 ± 2	46 ± 1
550	22 ± 2	64 ± 2	4 ± 1	79 ± 2	62 ± 6

Applied load of 100 MPa used in this study during sintering was sufficient not only to ensure relatively high density but pronounced deformation of the individual powder particles occurred as well. The microstructure of the sample compacted at 400 °C contained the highest volume fraction of small grains (<5 µm). Size of these grains, their distribution in the material and their volume fraction clearly indicate that they were formed during the sintering process. High strain applied to the material during the sintering resulted in deformation and application of high temperature consequently resulted in recrystallization. The degree of recrystallization was

directly proportional to the temperature used in the process; therefore, a continuous decrease of small grains fraction was observed with the increasing temperature. This conclusion is supported by other important attributes as well. The magnitude of residual stress, which is in this report qualitatively shown in KAM maps is quite high in the sample processed at the lowest temperature and decreases quickly with increasing sintering temperature. Recrystallization results in the transformation of the deformed structure into new, strain-free grains with high angle grain boundaries. Therefore, observed parameters such as HAGB fraction and fraction of grains with GOS <1.5° have opposite evolution as observed for the residual stress. However, an increase of average grain size, which often corresponds to the recrystallization degree, was not continuous. Its evolution was strongly affected by a broad distribution of the average grain size in the initial powder particles. Deformation and subsequently recrystallization occurred, especially along the former particle boundaries. Large grains present in the microstructure of the compacts were not completely consumed at lower temperatures and their presence led to an increase of the value of the average grain size calculated as an area fraction. As a result, the evolution of the mechanical strength as a function of the sintering temperature was significantly affected by residual stress, grain size and also coarsening of secondary phase particles.

4. CONCLUSIONS

Effect of the sintering temperature on the microstructure and mechanical properties was studied in AE42 magnesium alloy processed by spark plasma sintering. It was found that mechanical strength of the sintered samples was significantly affected by several microstructural features. The highest effect could be attributed to the grain growth and deformation hardening which occurred due to the relatively high load applied during sintering - 100 MPa. Sintering at 400 °C resulted only in partial recrystallization and the largest fraction of small grains (< 5 μm in diameter) was observed together with relatively high residual stress stored in the material. The increase of the sintering temperature resulted in more pronounced recrystallization and significant loss of mechanical properties occurred.

ACKNOWLEDGEMENTS

This work was financially supported by the Czech Science Foundation under the project GA18-19213Y.

REFERENCES

[1] BETTLES, C.J. Magnesium Powder Metallurgy: Process and Materials Opportunities. *Journal of Materials Engineering and Performance*. 2008. vol. 17, no. 3, pp. 297-301.

[2] STAIGER, M.P., PIETAK, A.M., HUADMAI, J. and DIAS, G. Magnesium and its alloys as orthopedic biomaterials: A review. *Biomaterials*. 2006. vol. 27, no. 9, pp. 1728-1734.

[3] MUNIR ZUHAIR A., QUACH DAT, V. and OHYANAGI, M. Electric Current Activation of Sintering: A Review of the Pulsed Electric Current Sintering Process. *Journal of the American Ceramic Society*. 2010. vol. 94, no. 1, pp. 1-19.

[4] GUAN, D., RAINFORTH, W.M., SHARP, J., GAO, J. and TODD, I. On the use of cryomilling and spark plasma sintering to achieve high strength in a magnesium alloy. *Journal of Alloys and Compounds*. 2016. vols. 688, Part A, pp. 1141-1150.

[5] MUHAMMAD, W.N.A.W., SAJURI, Z., MUTOH, Y. and MIYASHITA, Y. Microstructure and mechanical properties of magnesium composites prepared by spark plasma sintering technology. *Journal of Alloys and Compounds*. 2011. vol. 509, no. 20, pp. 6021-6029.

[6] MUHAMMAD, W.N.A.W., MUTOH, Y. and MIYASHITA, Y. Microstructure and mechanical properties of magnesium prepared by spark plasma sintering. *Advanced Materials Research*. 2010. vols. 129-131, pp. 764-768.

[7] STRAFFELINI, G., NOGUEIRA, A.P., MUTERLLE, P. and MENAPACE, C. Spark plasma sintering and hot compression behaviour of AZ91 Mg alloy. *Materials Science and Technology*. 2011. vol. 27, no. 10, pp. 1582-1587.

[8] BOTELHO, de O., AUGUSTO, P., STRAFFELINI, G. and MENAPACE, C. Spark plasma sintering and hot compression analysis of pure Mg and AZ91 alloy. *Materials Science Forum*. 2014. vol. 802, pp. 467-471.

[9] CHEN, Y.Y., YU, H.B., ZHANG, D.L. and CHAI, L.H. Effect of spark plasma sintering temperature on microstructure and mechanical properties of an ultrafine grained TiAl intermetallic alloy. *Materials Science and Engineering: A*. 2009. vol. 525, nos. 1-2, pp. 166-173.

[10] MÉAR, F.O., XIE, G., LOUZGUINE-LUZGIN, D.V. and INOUE, A. Spark plasma sintering of Mg-based amorphous ball-milled powders. *Materials Transactions*. 2009. vol. 50, no. 3, pp. 588-591.

[11] MINÁRIK, P., STRÁSKÝ, J., VESELÝ, J., LUKÁČ, F., HADZIMA, B. and KRÁL¸R. AE42 magnesium alloy prepared by spark plasma sintering. *Journal of Alloys and Compounds*. 2018. vol. 742, pp. 172-179.

[12] CHENG, Y., CUI, Z., CHENG, L., GONG, D. and WANG, W. Effect of particle size on densification of pure magnesium during spark plasma sintering. *Advanced Powder Technology*. 2017. vol. 28, no. 4, pp. 1129-1135.

[13] SON, H.T., HONG, J.M., OH, I.H. LEE, J.S., KIM, T.S. and MARUYAMA, K. Microstructure and mechanical properties of Mg-Zn-Y alloys fabricated by rapid solidification and spark plasma sintering processes. *Solid State Phenomena*. 2007. vols. 124-126, pp. 1517-1520.

[14] MINÁRIK, P., KRÁL, R., ČÍŽEK, J. and CHMELÍK, F. Effect of different c/a ratio on the microstructure and mechanical properties in magnesium alloys processed by ECAP. *Acta Materialia*. 2016. vol. 107, pp. 83-95.